Random Packings of Frictionless Particles

Corey S. O'Hern,[1,3] Stephen A. Langer,[2] Andrea J. Liu,[1] and Sidney R. Nagel[3]
[1]*Department of Chemistry and Biochemistry, UCLA, Los Angeles, California 90095-1569*
[2]*Information Technology Laboratory, NIST, Gaithersburg, Maryland 20899-8910*
[3]*James Franck Institute, The University of Chicago, Chicago, Illinois 60637*
(Received 31 October 2001; published 31 January 2002)

We conduct numerical simulations of random packings of frictionless particles at $T = 0$. The packing fraction where the pressure becomes nonzero is the same as the jamming threshold, where the static shear modulus becomes nonzero. The distribution of threshold packing fractions narrows, and its peak approaches random close packing as the system size increases. For packing fractions within the peak, there is no self-averaging, leading to exponential decay of the interparticle force distribution.

DOI: 10.1103/PhysRevLett.88.075507 PACS numbers: 81.05.Rm, 82.70.–y, 83.80.Fg

A system jams when it develops a yield stress or extremely long stress relaxation time in a disordered state [1]. Different control parameters can be varied to induce jamming, such as the temperature T, applied shear stress σ, or packing fraction ϕ, as shown in the phase diagram inset of Fig. 1(a) [2]. Such a phase diagram might apply, e.g., to supercooled liquids, granular materials, foams, and suspensions. For the diagram to be useful, there should be a common physical origin for jamming independent of the control parameter varied. Previously, it was shown [3] that the onset of a peak in the distribution of interparticle normal forces, $P(F)$, signifies the development of a yield stress in a variety of systems [4], implying that the jamming phase diagram is a useful concept.

There is a special point on the jamming phase diagram, marked J in Fig. 1(a), for repulsive, finite-range potentials. This point, at zero temperature and shear stress, represents the onset of jamming with increasing packing fraction. Static granular packings necessarily lie near this point because they are effectively at $T = 0$ (thermal energy is much smaller than the energy needed to lift a grain by its own diameter) and the particles are nearly hard, so it is difficult to compress packings further into the jammed region. Experimentally, $P(F)$ for granular packings has a remarkably robust form [5]; not only does it have a slight peak, but it also has an exponentially decreasing tail at large F. Numerous simulations find the same form for $P(F)$ [6,7]. The persistence of the exponential tail, independent of the potential, is surprising.

In this Letter, we quench systems of frictionless, repulsive particles from high temperature to $T = 0$ (and also $\sigma = 0$) near point J in the jamming diagram. Our simulations show that different configurations have different properties, even for arbitrarily large system sizes, so that self-averaging is not observed. However, the range of packing fractions over which self-averaging is not observed narrows with increasing system size. We will show that one consequence of non-self-averaging is an exponential decay of $P(F)$ at large F.

To create configurations near point J we start with random configurations (i.e., $T = \infty$) and, as with inherent structures [8], quench infinitely rapidly to $T = 0$ at fixed ϕ using conjugate gradient (CG) energy minimization with periodic boundary conditions [9]. In our simulations, we use 50:50 binary mixtures of N frictionless particles

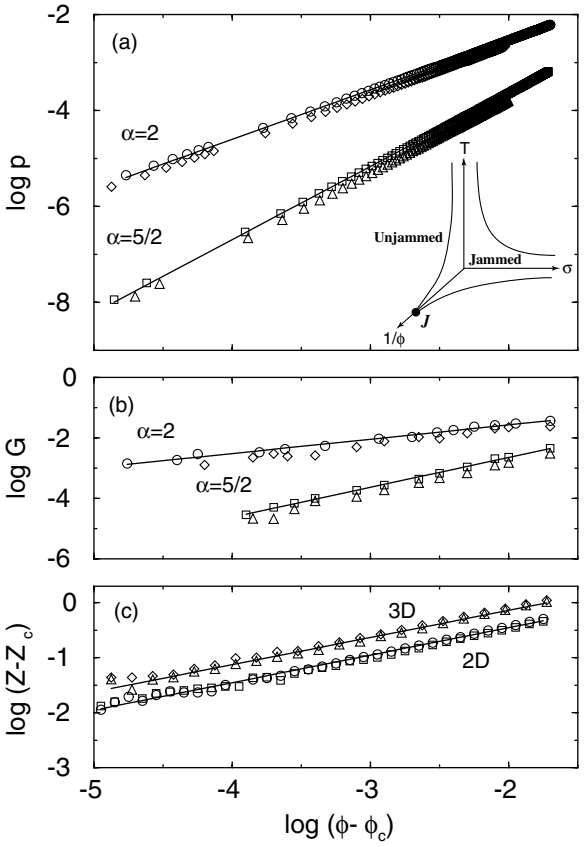

FIG. 1. (a) Pressure p vs $\phi - \phi_c$, where ϕ_c is the threshold packing fraction for a given state. Circles (squares) correspond to $\alpha = 2(5/2)$ in 2D and diamonds (triangles) correspond to $\alpha = 2(5/2)$ in 3D and $N = 1024(512)$ in 2D (3D). Inset: Jamming phase diagram showing onset of jamming at point J. (b) Shear stress G vs $\phi - \phi_c$. The shear strain is applied in the x direction, the strain gradient is in the y direction, and the xy component of the stress tensor is measured. (c) Number of overlaps per particle $Z - Z_c$ vs $\phi - \phi_c$.

with a diameter ratio 1.4 [10,11] that interact pairwise via repulsive potentials: $v_{ab}(r) = (\epsilon/\alpha)(1 - r/\sigma_{ab})^{\alpha}$ for $r < \sigma_{ab}$ and $v_{ab}(r) = 0$ for $r > \sigma_{ab}$, where a, b label particles and $\sigma_{ab} = (\sigma_a + \sigma_b)/2$. We study harmonic ($\alpha = 2$) and Hertzian ($\alpha = 5/2$) potentials in 2D and 3D. The total potential energy is $V = 0$ if no particles overlap. Energy is measured in units of ϵ and length in units of the small particle diameter σ_1.

We classify each final configuration as either overlapped ($V \neq 0$) or nonoverlapped ($V = 0$). Overlapping configurations have a nonzero pressure, p, while nonoverlapping ones have $p = 0$. The virial expression is used to calculate p [12]. Is a configuration that has $p > 0$ necessarily jammed with a static shear modulus $G > 0$? To answer this question, we study states close to overlap threshold as a function of ϕ. We find the overlap threshold, ϕ_c, for each configuration by compressing a nonoverlapped state while measuring p. After each small increment in ϕ ($\delta\phi \leq 10^{-4}$), we use CG to bring the state to the lowest energy attainable without crossing any barriers. (To check that no barriers were crossed, we reproduced our results using 10 times smaller increments in ϕ.) This procedure allows us to measure zero-frequency properties of the system.

Different states have different values of the overlap threshold, ϕ_c. Nevertheless, when we plot pressure p versus $\phi - \phi_c$ [Fig. 1(a)], the results for different configurations collapse on a single curve. This holds for harmonic ($\alpha = 2$) and Hertzian ($\alpha = 5/2$) potentials in 2D and 3D. We find $p = p_0(\phi - \phi_c)^{\beta}$, where p_0 is only weakly dependent on dimension and $\beta = 1.0$ for $\alpha = 2$ and $\beta = 1.5$ for $\alpha = 5/2$ in 2D and 3D. This is consistent with previous results at larger $\phi - \phi_c$ [6,13,14]. To see if states with $p > 0$ are jammed, we calculate the shear modulus, G, by applying a small step strain and measuring the infinite-time response by minimizing the energy using CG. The response is linear for sufficiently small strains. Figure 1(b) shows that $G = G_0(\phi - \phi_c)^{\gamma}$, where $\gamma = 0.5$ for $\alpha = 2$ [13], and $\gamma = 1.0$ for $\alpha = 5/2$, in 2D and 3D. To our resolution, which is better than 10^{-4}, we find that G and p vanish at the same packing fraction ϕ_c. Thus, the onset of jamming, as defined in the first paragraph, coincides with the onset of overlap [15].

When a configuration jams at ϕ_c, the number of overlaps per particle, Z, jumps from zero to a threshold value Z_c. Above ϕ_c, Z increases as $Z - Z_c = Z_0(\phi - \phi_c)^{\zeta}$, as shown in Fig. 1(c). For both harmonic and Hertzian potentials, we find $\zeta = 0.5$ in both 2D and 3D [13]. (If there are no zero-energy modes, $Z_c = 2d$ for frictionless spheres in d dimensions [1]. Usually $\approx$5% of particles are "rattlers" that do not overlap with any neighbors. If we remove these, we find $Z_c = 2d$.)

By studying the onset of jamming in repulsive systems at $T = 0$, we have a criterion for whether a state is jammed or not (i.e., $V > 0$ or $V = 0$). If there is a packing with $V = 0$, then it is an equilibrium configuration. The state that maintains $V = 0$ up to the highest ϕ is therefore the one that, when compressed infinitesimally above this point, becomes the zero-temperature equivalent to the ideal glass. We have found that the properties shown in Fig. 1 depend only on $\phi - \phi_c$. This suggests that this behavior is the same as for the ideal glass.

Although Fig. 1 shows scaling behavior above ϕ_c, the value of ϕ_c varies from state to state. How much can ϕ_c vary? Our protocol of starting with random configurations and quenching infinitely rapidly to $T = 0$ should, in principle, allow us to sample all of phase space. For each ϕ, we measure the fraction of initial states that lead to jammed states at $T = 0$. Figure 2(a) shows the probability, $f_j(\phi)$, of finding a jammed state for different system sizes in 3D for the harmonic potential. For each N, we have differentiated f_j with respect to ϕ to obtain the probability distribution $P_j(\phi_c)$ of finding a jamming threshold of ϕ_c [see Fig. 2(b)]. System size has a large effect. For each N, we characterize $P_j(\phi_c)$ by its full width at half maximum, w, and its peak position, ϕ_0. Figure 2(c) shows that, for $N > 10$, $w \propto N^{-\omega}$, where $\omega \approx 0.55$. Similarly, Fig. 2(d) shows that ϕ_0 approaches its

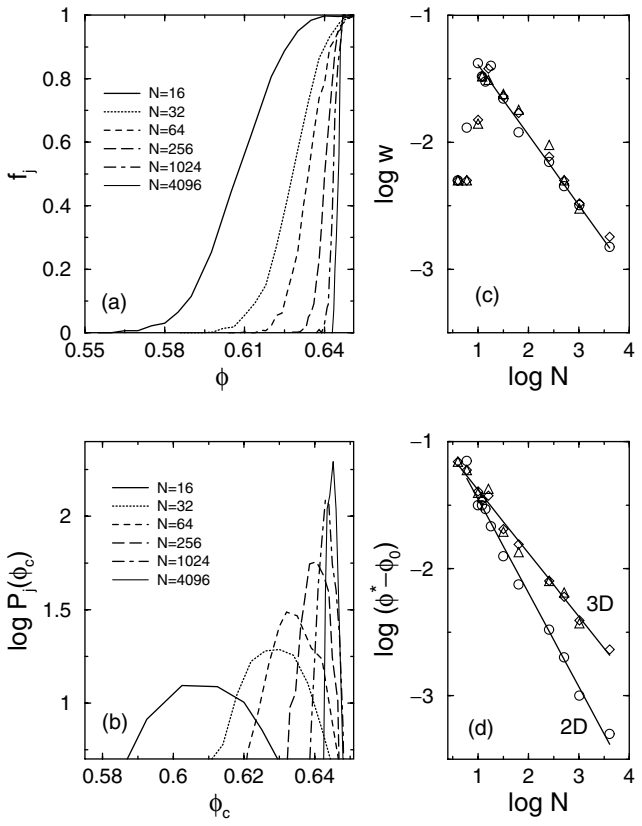

FIG. 2. (a) The probability f_j of finding a jammed state vs ϕ for $\alpha = 2$ in 3D and several system sizes, N. (b) The probability distribution $P_j(\phi_c)$ of finding a jamming threshold ϕ_c for systems considered in (a). (c) Full width at half maximum w of $P_j(\phi_c)$ vs N. (d) The deviation in peak position ϕ_0 of $P_j(\phi_c)$ from its asymptotic value ϕ^* vs N. Data for (c) and (d) are for systems considered in Fig. 1 except $\alpha = 5/2$ in 2D.

asymptotic value ϕ^* as $\phi^* - \phi_0 \propto N^{-\theta}$, where $\theta \approx 0.7$ for 2D and $\theta \approx 0.5$ for 3D. We find $\phi^* = 0.842$ in 2D and $\phi^* = 0.648$ in 3D, close to well-known values of random close packing [16].

For finite N, the peak ϕ_0 of the distribution $P_j(\phi_c)$ corresponds to the largest number of initial states that lead to final jammed states (not the largest number of distinct final jammed states). ϕ_0 is a measure of the largest fraction of phase space that leads to the onset of jamming for a given N. ϕ^* thus represents where the jamming threshold is maximally random in the $N \to \infty$ limit. We find the same limiting value of ϕ^* for Hertzian and harmonic potentials, suggesting that ϕ^* is not sensitive to the potential. We can approach jammed hard-sphere packings by noting that states up to the jamming threshold are accessible to hard spheres. If we repeat the measurement of ϕ^* for potentials with progressively harder repulsions, we can approach (but not attain) the hard-sphere limit. This suggests a way to measure the maximally random jammed packing fraction for hard spheres [17].

It is well known that spherical granular materials can exist over a 15% spread of packing fractions from 0.55 to 0.64 [18,19]. The width of $P_j(\phi_c)$ for isotropic packings of frictionless particles is a maximum near $N = 10$ and becomes arbitrarily small when $N \to \infty$. Only for $N \approx 10$ can we find jammed states as low as $\phi = 0.55$. Thus, the experimental difference between loose and close packing cannot be explained simply by considering allowed configurations of frictionless spheres; the value of loose packing is not a purely geometrical quantity.

There are other protocols for finding the jamming threshold at $T = 0$. We have also generated configurations by cooling slowly from equilibrium thermal states to $T = 0$. In that case, we find that $P_j(\phi_c)$ is shifted to higher values of ϕ_c, with values of ϕ_0 that are less than 1% higher than for the first protocol, but it is difficult to determine whether the difference persists when $N \to \infty$.

We have shown that as $N \to \infty$ the range of packing fractions over which systems can jam becomes arbitrarily narrow. Therefore, one might suppose that the fact that different configurations jam at different packing fractions might become irrelevant in the large N limit. This is not the case because within the range over which both jammed and unjammed configurations exist, there is no self-averaging. For example, if a configuration is unjammed, with $V = 0$ every subset of that configuration has $V = 0$ as well. Less obvious is that for jammed configurations all subsets of more than a few particles will likely also contain overlaps. This is found numerically, and stems from the fact that, on average, each jammed particle must have at least $2d$ overlapping contacts, each of which also has $2d$ contacts. This constraint makes it unlikely that a jammed system can exist with pockets containing more than a few rattlers.

The distribution of interparticle normal forces, $P(F)$, illustrates the absence of self-averaging. Simulations of static packings [6,7] have shown that, at large F, $P(F)$ falls off exponentially even for harmonic and Hertzian potentials. An argument based on equilibrium liquids [3], however, suggests that the distribution should fall off differently for different potentials: the large force tail depends on the pair-distribution function at small r, which in equilibrium varies approximately as $\exp[-V(r)/kT]$. By this reasoning, one would predict a Gaussian tail for $P(F)$ for a harmonic potential. Indeed, we do find a Gaussian tail except at $T = 0$ near ϕ_0 [the peak of $P_j(\phi_c)$], where both jammed and unjammed configurations can exist. In this region, we obtain a different result for $P(F)$, depending on whether we scale F by its average value before or after taking the configurational average. If, for each configuration, the forces F are scaled by the average value *for that configuration*, $\langle F \rangle$, and the resulting distribution $P(F/\langle F \rangle)$ is then averaged over all configurations, the result is as shown in Fig. 3(a). On the other hand, if the forces are scaled by the average over *all* configurations, $\langle\langle F \rangle\rangle$, the resulting $P(F/\langle\langle F \rangle\rangle)$ is as shown in Fig. 3(b). We see that at $\phi = 0.644$, near the peak of $P_j(\phi_c)$ for $N = 1024$, the high force tail falls off much more slowly in this latter case than in the former, where each configuration is averaged separately. As the packing fraction is increased above ϕ_c, there is less difference between the curves $P(F/\langle\langle F \rangle\rangle)$ and $P(F/\langle F \rangle)$. This trend can be explained since, near ϕ_c, $\langle F \rangle$ varies dramatically from configuration to configuration. The relative size of fluctuations in $\langle F \rangle$ decreases with increasing ϕ, and the exponential decay of $P(F)$ thus disappears. As the size of the system increases, the width of the region in ϕ over which the high-force tail is exponential will decrease. However, one can always tune ϕ close enough to ϕ_0 to observe the exponential tail.

The shape of the tail of $P(F/\langle\langle F \rangle\rangle)$ can be computed analytically, given a few simple assumptions. We have found that the average force in a configuration, $\langle F \rangle$, is proportional to the pressure p at $T = 0$ near the onset of jamming. So from Fig. 1(a), we know that

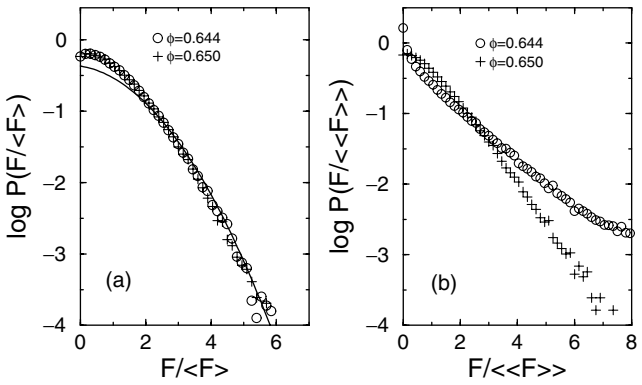

FIG. 3. (a) Force distribution $P(F/\langle F \rangle)$ obtained by scaling F by the average force $\langle F \rangle$ of each configuration using the harmonic potential in 3D with $N = 1024$. The solid line is a Gaussian fit to the high-force tail. (b) Same as (a) except F is scaled by $\langle\langle F \rangle\rangle$ averaged over all configurations.

$\langle F\rangle = F_0(\phi - \phi_c)$ for the harmonic potential. We assume that the jamming threshold, ϕ_c, is distributed as a Gaussian centered at ϕ_0 with width w as found in Fig. 2(b). Finally, we assume [as shown in Fig. 3(a)] that the tail of $P(F/\langle F\rangle)$ for individual configurations is given by the equilibrium argument, which implies a Gaussian tail centered at $F/\langle F\rangle = 0$ with width σ_F. (Here F_0, σ_F, ϕ_0, and w are parameters that can be obtained from the simulation data.) In the large F limit, we find

$$P(F) \propto \int_0^{\phi} d\phi_c \, \frac{1}{\langle F\rangle} e^{-F^2/(2\langle F\rangle^2\sigma_F^2)} e^{-(\phi_c-\phi_0)^2/(2w^2)} \quad (1)$$

$$\approx \frac{\exp(-F/\langle\langle F\rangle\rangle)}{\sqrt{F/\langle\langle F\rangle\rangle}}. \quad (2)$$

We have also studied Hertzian potentials and find results similar to those for the harmonic potential shown in Fig. 3 and Eq. (2). In experimental granular systems, where the interparticle potential is expected to be Hertzian at contact, $P(F)$ has an exponential tail even for a single configuration [5]. We speculate that this is due to friction in the laboratory system, which allows heterogeneities from region to region within a single sample.

We have shown that for a finite-size system the jamming phase diagram looks somewhat different from the one sketched in the inset of Fig. 1(a). Instead of a well-defined point J, we find that there is a region of ϕ, centered around ϕ_0 with width w, in which both jammed and unjammed states can exist. As the size of the system increases, this region shrinks to the point J. Effects not included in our simulations, such as the presence of friction, nonspherically symmetric potentials, or anisotropic packing (such as sequential packing under gravity) may prevent this region from disappearing.

In some ways, point J in the phase diagram resembles a critical point: there is power-law scaling (Fig. 1), $P(F/\langle\langle F\rangle\rangle)$ has a robust exponential tail independent of potential, and configurations are not self-averaging. In the context of foam, it has also been speculated that point J corresponds to rigidity percolation [20]. However, near J the behavior differs from ordinary critical behavior, where configurations are not self-averaging once the correlation length exceeds the system size. There are no fluctuations near J; that is, an unjammed (jammed) configuration will be unjammed (jammed) everywhere. This, as well as the fact that no bonds exist at packing fractions below J, makes this transition also different from rigidity percolation. Moreover, even though we find power laws near J, there is a jump from $Z = 0$ to $Z = Z_c$, and the exponents depend on the potential but not on dimension. Thus, point J has rather special properties.

We thank J.-P. Bouchaud, P. Chaikin, D. Durian, G. Grest, D. Levine, J. Socolar, and T. Witten for helpful discussions. We acknowledge support from NSF-DMR-0089081 (C.S.O., S.R.N.) and DMR-0087349 (C.S.O., A.J.L.) and computing resources from the High Performance Computing Research Facility at Argonne National Lab.

[1] See *Jamming and Rheology,* edited by A. J. Liu and S. R. Nagel (Taylor & Francis, New York, 2001), and references therein.
[2] A. J. Liu and S. R. Nagel, Nature (London) **396**, 21 (1998).
[3] C. S. O'Hern, S. A. Langer, A. J. Liu, and S. R. Nagel, Phys. Rev. Lett. **86**, 111 (2001).
[4] The peak in $P(F)$ is more generally indicative of a yield stress, and appears also in crystals and 1D chains.
[5] D. M. Mueth, H. M. Jaeger, and S. R. Nagel, Phys. Rev. E **57**, 3164 (1998); D. L. Blair, N. W. Mueggenburg, A. H. Marshall, H. M. Jaeger, and S. R. Nagel, Phys. Rev. E **63**, 041304 (2001).
[6] H. A. Makse, D. L. Johnson, and L. M. Schwartz, Phys. Rev. Lett. **84**, 4160 (2000).
[7] F. Radjai, M. Jean, J.-J. Moreau, and S. Roux, Phys. Rev. Lett. **77**, 274 (1996); C. Thornton, Kona Powder and Particle **15**, 103 (1997); M. L. Nguyen and S. N. Coppersmith, Phys. Rev. E **62**, 5248 (2000).
[8] F. H. Stillinger and T. A. Weber, Science **225**, 983 (1984).
[9] W. H. Press, B. P. Flannery, S. A. Teukolsky, and W. T. Vetterling, *Numerical Recipes in Fortran 77* (Cambridge University Press, New York, 1986).
[10] R. J. Speedy, J. Chem. Phys. **110**, 4559 (1999).
[11] D. N. Perera and P. Harrowell, Phys. Rev. E **59**, 5721 (1999).
[12] M. P. Allen and D. J. Tildesley, *Computer Simulation of Liquids* (Oxford University Press, New York, 1987).
[13] D. J. Durian, Phys. Rev. Lett. **75**, 4780 (1995); Phys. Rev. E **55**, 1739 (1997).
[14] T. G. Mason, M.-D. Lacasse, G. S. Grest, D. Levine, J. Bibette, and D. A. Weitz, Phys. Rev. E **56**, 3150 (1997).
[15] This result suggests that states at ϕ_c are not "fragile," as in M. E. Cates, J. P. Wittmer, J.-P. Bouchaud, and P. Claudin, Phys. Rev. Lett. **81**, 1841 (1998). It is possible that states below ϕ_c can jam when a shear stress is applied. Such states can support a pressure but are fragile because they will yield when the shear stress is reversed.
[16] J. G. Berryman, Phys. Rev. A **27**, 1053 (1983); A. S. Clarke and J. D. Wiley, Phys. Rev. B **35**, 7350 (1987).
[17] S. Torquato, T. M. Truskett, and P. G. Debenedetti, Phys. Rev. Lett. **84**, 2064 (2000).
[18] J. D. Bernal, Nature (London) **188**, 910 (1961); J. D. Bernal, J. Mason, and K. R. Knight, Nature (London) **194**, 956 (1962).
[19] G. Y. Onoda and E. G. Liniger, Phys. Rev. Lett. **64**, 2727 (1990).
[20] F. Bolton and D. Weaire, Phys. Rev. Lett. **65**, 3449 (1990); D. J. Jacobs and M. F. Thorpe, Phys. Rev. E **53**, 3682 (1996).